JACS
JOURNAL OF THE AMERICAN CHEMICAL SOCIETY
Article
pubs.acs.org/JACS

Interception and Characterization of Catalyst Species in Rhodium Bis(diazaphospholane)-Catalyzed Hydroformylation of Octene, Vinyl Acetate, Allyl Cyanide, and 1-Phenyl-1,3-butadiene

Eleanor R. Nelsen,[†,‡] Anna C. Brezny,[‡] and Clark R. Landis*

Department of Chemistry, University of Wisconsin-Madison, 1101 University Avenue, Madison, Wisconsin 53706, United States

Supporting Information

ABSTRACT: In the absence of H_2, reaction of [Rh(H)$(CO)_2$(BDP)] [BDP = bis(diazaphospholane)] with hydroformylation substrates vinyl acetate, allyl cyanide, 1-octene, and *trans*-1-phenyl-1,3-butadiene at low temperatures and pressures with passive mixing enables detailed NMR spectroscopic characterization of rhodium acyl and, in some cases, alkyl complexes of these substrates. For *trans*-1-phenyl-1,3-butadiene, the stable alkyl complex is an η^3-allyl complex. Five-coordinate acyl dicarbonyl complexes appear to be thermodynamically preferred over the four-coordinate acyl monocarbonyls at low temperatures and one atmosphere of CO. Under noncatalytic (i.e., no H_2 present) reaction conditions, NMR spectroscopy reveals the kinetic and thermodynamic selectivity of linear and branched acyl dicarbonyl formation. Over the range of substrates investigated, the kinetic regioselectivity observed at low temperatures under noncatalytic conditions roughly predicts the regioselectivity observed for catalytic transformations at higher temperatures and pressures. Thus, kinetic distributions of off-cycle acyl dicarbonyls constitute reasonable models for catalytic selectivity. The Wisconsin high-pressure NMR reactor (WiHP-NMRR) enables single-turnover experiments with active mixing; such experiments constitute a powerful strategy for elucidating the inherent selectivity of acyl formation and acyl hydrogenolysis in hydroformylation reactions.

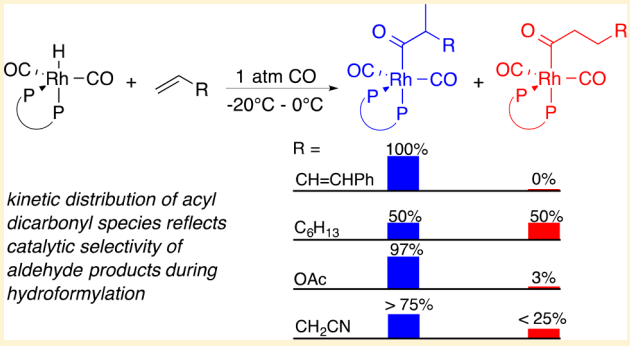

INTRODUCTION

Since its discovery more than 75 years ago, the hydroformylation of alkenes (see Scheme 1) has become one of the largest-scale applications of homogeneous catalysis in industry.[1] Rhodium complexes modified with phosphorus-based ligands yield highly active and selective catalysts, facilitating the production of millions of tons per year of aldehydes—predominantly the linear product, a versatile feedstock for the production of other commodity chemicals.

Scheme 1. Hydroformylation of Alkenes

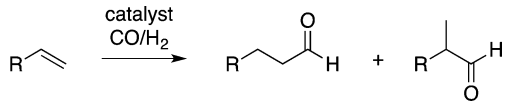

The comparatively underdeveloped asymmetric reaction shows promise for enantiopure chemical production, because chiral aldehydes are attractive precursors for pharmaceutical and other fine-chemical products.[2] Broad application of hydroformylation in the synthesis of chiral molecules depends on the ability to control both regio- and enantioselectivity. The last two decades have seen considerable activity in the development of new ligands for asymmetric hydroformylation (AHF).[3] The 3,4-bis(diazaphospholane) (BDP) class of ligands introduced in 2004 combine high activity—greater than one turnover per second—and useful selectivities for the enantioselective hydroformylation of various alkene substrates (Figure 1).[4]

The general mechanism for hydroformylation was proposed by Heck and Breslow for cobalt-catalyzed hydroformylation some 50 years ago (see Scheme 2), and remains accepted today.[5] Our ultimate goal is to understand how the kinetic and

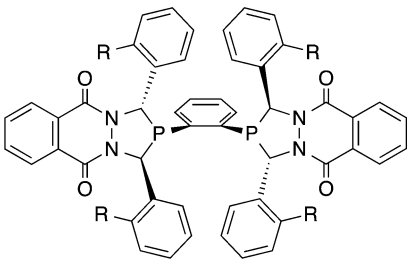

Figure 1. Structure of (*S*,*S*)-3,4-bis(diazaphospholane) (BDP). This work uses *rac* BDP with R = H.

Received: September 18, 2015
Published: October 15, 2015

DOI: 10.1021/jacs.5b09858
J. Am. Chem. Soc. 2015, 137, 14208−14219

Scheme 2. General Mechanism for Hydroformylation

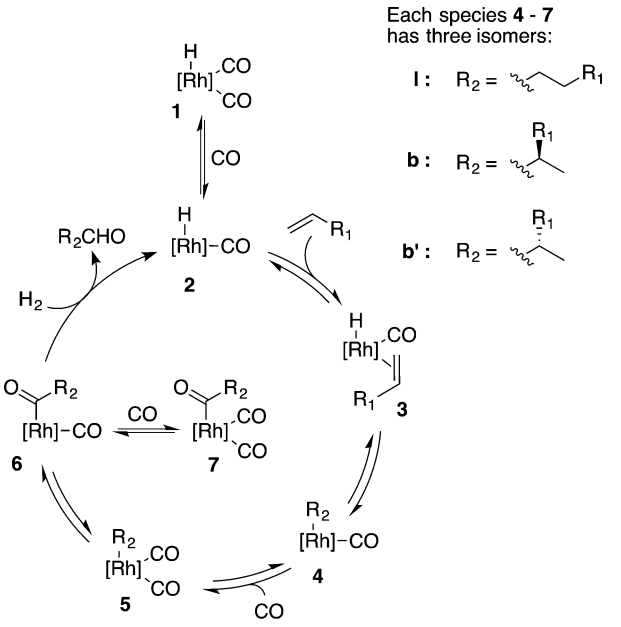

thermodynamic selectivities of the individual steps of this mechanism influence the net regio- and enantioselectivity of AHF and their responses to reaction conditions.

One empirical approach to elucidating the origins of selectivity in a catalytic reaction involves the detailed determination of rate laws for the formation of all products over a wide variety of reaction conditions. From such empirical data the mechanistic step, or collections of steps, that control(s) selectivity may be inferred; we call this an outside-in approach. The level of detail of the mechanistic inference depends on the complexity of the observed rate laws, with more complex rate laws possessing greater intrinsic information. Additional information may be extracted from the distributions of isotopic labels as a function of reaction conditions. Many such studies have been performed for nonenantioselective hydroformylation reactions with mono- or bidentate phosphorus ligands.[6] For the AHF of styrene with Rh(BDP) catalysts we have reported empirical rate laws over a wide variety of reaction pressures.[7]

The other empirical extreme for elucidation of detailed catalytic mechanisms concerns isolating and characterizing key intermediates and examining their kinetic and thermodynamic properties. If enough of these intermediates and their properties can be studied, the origins of selectivity can be deduced. This may be called an inside-out approach because understanding of what comes out of a catalytic cycle is revealed by direct observation of what lies inside the cycle. Few studies report direct characterization of the intermediates in useful hydroformylation reactions. Brown and Kent's pioneering NMR studies of the reaction of styrene with $[Rh(H)(CO)(PPh_3)_3]$, the catalyst precursor and resting state, revealed formation of branched and linear acyls of the formula $Rh(acyl)(PPh_3)_2(CO)_2$, with the branched acyl formed first and followed by equilibration to the more stable linear acyl.[8] Since that time, however, there have been few cases of observation of catalyst species,[9] and most of these have been limited to slow and/or unselective catalysts[10] or synthesis of analogous iridium complexes.[11−13] Previously, we examined the reaction of $[Rh(H)(BDP)(CO)_2]$ with styrene in the absence of H_2 and reported the first interception of linear and branched rhodium alkyl, as well as acyl, intermediates in AHF (see Chart 1). These intermediates were characterized by multinuclear

Chart 1. Alkyl and Acyl Rhodium Bis(diazaphospholane) Complexes Identified Following the Reaction of 1 with Styrene

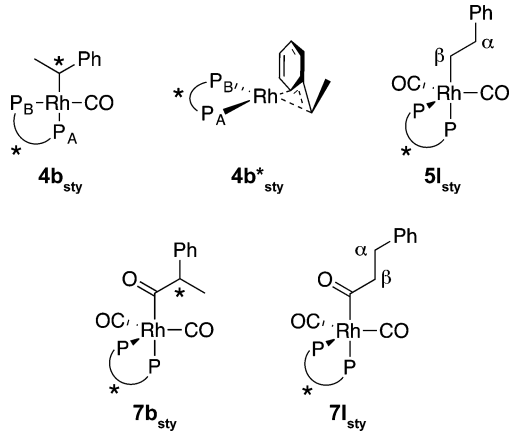

NMR spectroscopy, their relative thermodynamic stabilities were estimated,[14] and we demonstrated that the thermodynamic preference for linear versus branched isomers inverts upon conversion of the rhodium alkyls to the rhodium acyls.

The most complete understanding of the origins of selectivity in a catalytic reaction comes from a combination of outside-in and inside-out approaches. For example, direct observation of catalyst resting state by *operando* spectroscopic methods provides an invaluable check on the interpretation of empirical rate laws.

This paper comprises two major sections. Following a brief presentation of some benchmarking catalytic results, the first section reports the interception and NMR characterization of catalytic intermediates that include common substrates for AHF: vinyl acetate, allyl cyanide, 1-octene, and *trans*-1-phenyl-1,3-butadiene. Such data provide an essential foundation for more in-depth analysis of kinetic and thermodynamic selectivity in AHF. The conditions of these experiments, low temperature and decreasing concentrations of dissolved CO, enable characterization of species such as Rh-alkyls and Rh-acyl monocarbonyls that are not generally accessible. However, these conditions are very different from those of actual catalysis. The second major section of this work applies high-pressure NMR techniques to probe (1) the equilibration of Rh-allyls and acyl dicarbonyl intermediates for the hydroformylation of *trans*-1-phenyl-1,3-butadiene and (2) the interplay of kinetic and thermodynamic selectivity for the formation of linear and branched acyl intermediates and their hydrogenolysis.

RESULTS AND DISCUSSION

The alkenes chosen for this study are all monosubstituted but span a modest range of substituent electronic effects, from electron-withdrawing in the σ bond framework (vinyl acetate) to electron-donating (1-octene). Styrene, vinyl acetate, and allyl cyanide appear to be intrinsically selective for the branched product under common reaction conditions. For the tetraphenyl BDP catalyst (Figure 1, R = H), the catalytic selectivities are reported under standard (150 psi CO/H_2, 75 °C) and low-temperature conditions (30 psi CO/H_2, 0 °C)

DOI: 10.1021/jacs.5b09858
J. Am. Chem. Soc. 2015, 137, 14208−14219

Table 1. Selectivities for Catalytic AHF under Two Different Sets of Conditions for Four Substrates with the Tetraphenyl BDP Catalyst

	150 psi CO/H_2, 75 °C		30 psi CO/H_2, 0 °C
substrate	regioselectivity	ee	regioselectivity[a]
vinyl acetate	b:l = 13.1[b]	14[b]	b:l = 49
allyl cyanide	b:l = 4.9[b]	65.8[b]	b:l = 12
phenyl-butadiene	60% 3-formyl product[c]	n.d.[d]	only 3-formyl product obsd
1-octene	b:l = 0.66[b]	n.d	b:l = 0.92

[a]Based on ^{1}H NMR spectroscopy. [b]Jerry Klozin, Dow Chemical Company, 2004. [c]Other products correspond to double-bond isomers of primary product. [d]n.d.: not determined.

(Table 1). Catalytic reactions at low temperatures and pressures (relevant to this work) give higher selectivity toward the branched products than reactions under more common conditions (see Table 1). Dienes such as 1-phenyl-1,3-butadiene are selective for the branched 3-formyl-1-phenyl-1-butene product.[4e] A π-allyl complex (analogous to **4b***$_{sty}$) was proposed as an intermediate in this mechanism.

Simple alkenes such as 1-octene commonly favor the linear product. For example, 1-octene hydroformylation with the tetraphenyl BDP catalyst under the same conditions cited above yields b:l = 0.66.[15] Common rationalizations for regioselectivity in AHF invoke a general steric preference for the linear aldehyde that can be overridden by electronic factors. Thus, the high branched selectivity for electron-deficient olefins results from stabilization of branched alkyl complexes **4** by the electron-withdrawing substituents. In these species, the methine carbon, metal center, and trans phosphorus atom comprise a three-center, four-electron bond in which the phosphorus atom pushes electron density onto the alkyl carbon. For substrates like styrene, the EWG mitigates charge buildup on that carbon, stabilizing the branched alkyl species. The alkyl chain of 1-octene has the opposite effect, destabilizing **4b**$_{oct}$ relative to **4l**$_{oct}$ and reinforcing the steric preference for linear insertion.

Noncatalytic Experiment Description. *Noncatalytic* experiments in the absence of dihydrogen under low temperature and pressure conditions (−20 to 0 °C, 15 psia CO) proceed from RhH(BDP) $(CO)_2$ to the acyl dicarbonyls (**7b**$_{sty}$ and **7l**$_{sty}$) but cannot go on to aldehyde products. With passive mixing (i. e., unstirred or diffusive), only, in these experiments the total dissolved CO concentration is not known and changes significantly during the reaction. Reactions performed with active gas−liquid mixing (using WiHP-NMRR, *vide infra*) will be referred to as actively mixed. There are advantages and disadvantages of experiments run under low-temperature, passively mixed conditions. The low temperature and absence of H_2 enable direct observation of the formation of various acyl and, in some cases, alkyl isomers on convenient time scales.[16] These intermediates persist, under these conditions, sufficiently long for detailed characterization. However, it is not clear how the kinetic and thermodynamic selectivities obtained at low pressure and temperature with passive mixing relate to catalytic conditions.

Preliminary experiments (see Figure S1 in Supporting Information) for the reaction of [Rh(H)(BDP)$(CO)_2$] and alkene at −10 °C and 15 psi CO revealed different apparent half-lives for the four substrates: ca. 2 min (1-octene), 4 min (allyl cyanide), 18 min (vinyl acetate), and 30 min (*trans*-1-phenyl-1,3-butadiene). Because the rates vary so much, detailed analysis of thermodynamic and kinetic selectivity required different temperatures for different substrates. In all reactions, good (>90%) mass balance was observed as demonstrated in Figures S2−S5 in Supporting Information.

Vinyl Acetate. The reaction of vinyl acetate with rhodium hydride **1** at −10 °C under a CO atmosphere can be monitored easily by ^{1}H and ^{31}P NMR spectroscopy. As seen with styrene, **1** disappears over the course of 30 min to yield five-coordinate acyl dicarbonyl species (see Figure 2). The qualitative half-life

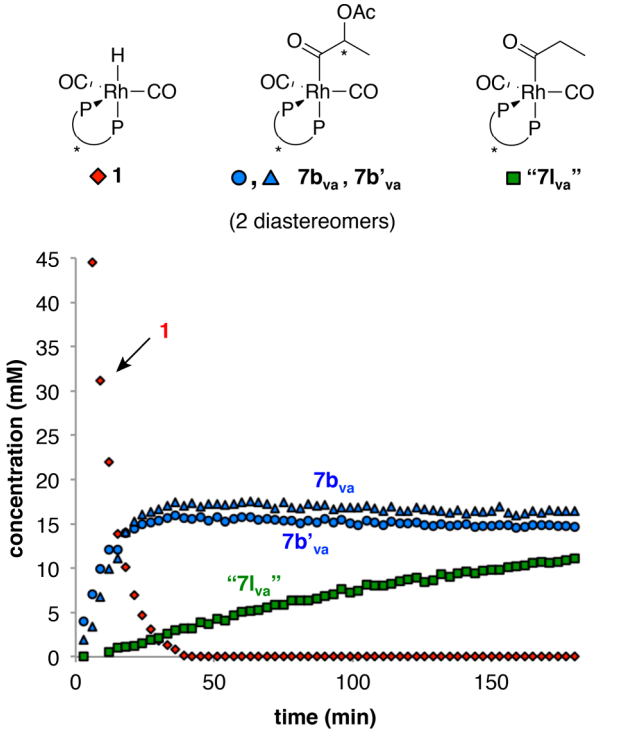

Figure 2. Catalyst speciation following the reaction of **1** (red diamonds) with vinyl acetate; the remaining mass balance comprises alkyl complexes (vide infra) (−10 °C, 15 psia CO, 65 mM **1**, 320 mM vinyl acetate, CH_2Cl_2). For plots demonstrating total mass balance, see Supporting Information.

of the disappearance of **1** is approximately 10 min. However, exact rates and kinetics are not perfectly reproducible due to the inconstant and unknown concentration of dissolved CO in a passively mixed standard NMR tube during reactions in which CO is consumed.

The diastereomeric branched acyl species **7b**$_{va}$ and **7b**′$_{va}$ appear as eight-line patterns in the ^{31}P{^{1}H} NMR spectrum at δ 69.5, 60.4 ppm and δ 68.5, 57.8 ppm, respectively. Another acyl species "**7l**$_{va}$" is responsible for the eight-line patterns at δ 70.1, 62.4 ppm (see Table S1 for complete NMR data), and increases in concentration over a longer time period than the branched acyls (see Figure 2). As the signal for "**7l**$_{va}$" grows in, the

DOI: 10.1021/jacs.5b09858
J. Am. Chem. Soc. 2015, 137, 14208−14219

catalyst precursor [Rh(acac)(BDP)] forms at the same rate and the alkyl species, **4b**$_{va}$, **4b***$_{va}$, and **5b**$_{va}$, disappear from solution (Figure 3).

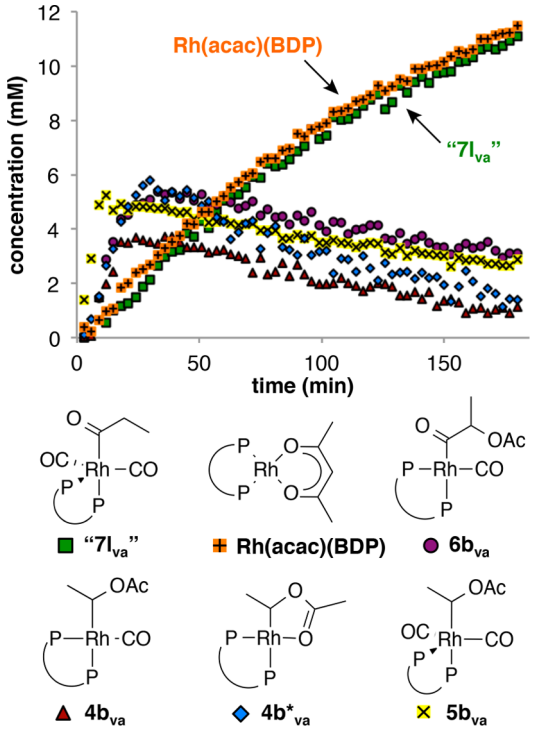

Figure 3. Disappearance of observed Rh-alkyl species and formation of "7l$_{va}$" and [Rh(acac)(BDP)] during reaction of **1** with vinyl acetate under the same conditions previously reported (−10 °C, 15 psia CO, 65 mM **1**, 320 mM vinyl acetate, CH_2Cl_2).

Characterization of Acyl Complexes. $^{31}P-^{1}H$ HMBC experiments show through-bond coupling from each set of ligand phosphorus atoms of **7b**$_{va}$ and **7b′**$_{va}$ to methine quartets and methyl doublets in the ^{1}H NMR spectrum. This experiment also revealed that, notably, *the linear acyl complex "7l$_{va}$" is not the β-acetoxypropionyl complex as expected, but the unsubstituted propionyl species* (see Figure 2). The HMBC spectrum shows correlations to two diastereotopic methylene protons at δ 2.62 and 1.67 ppm, as expected, but a COSY spectrum shows that these protons, rather than being correlated to an adjacent methylene group, are vicinal instead to a methyl group, which appears as a triplet at δ 0.5 ppm ($^{1}H-^{13}C$ HSQC shows that these protons are attached to a carbon atom with a signal at 10 ppm, also consistent with a methyl group). Thus, the linear acyl dicarbonyl "7l$_{va}$" appears to result from the reaction of ethene with **1** (*vide infra*).

A variety of other one- and two-dimensional NMR experiments, including $^{31}P-^{31}P$ COSY and $^{13}C-^{1}H$ HSQC, corroborate these assignments of **7b**$_{va}$ and **7b′**$_{va}$ as five-coordinate, branched acyl dicarbonyl complexes. The methine carbons of **7b**$_{va}$ and **7b′**$_{va}$ are visible at δ 86.2 and 83.9 ppm, respectively. The acyl and terminal carbonyl carbons of these complexes are also observable; chemical shifts and coupling constants are similar to those reported for complexes **7**$_{sty}$. The coordination number of complexes **7b**$_{va}$ and **7b′**$_{va}$ was determined by labeling with ^{13}CO; the upfield ^{31}P signal (P_{eq}) shows three new $^{1}J_{PC}$, consistent with an acyl dicarbonyl. The J_{PRh} values for these complexes—81 and 152 Hz for **7b**$_{va}$ and 80 and 167 Hz for **7b′**$_{va}$—are consistent with five-coordinate trigonal bipyramidal species.

The characterization of these off-cycle species raises the question: is the observation of these intermediates relevant to catalysis? The significance of the observation of these off-cycle species under low temperature, noncatalytic conditions is that it enables the kinetic selectivity of acyl dicarbonyl formation to be correlated with the product selectivity under catalytic conditions. For example, high branched selectivity for formation of acyl dicarbonyls mirrors the high selectivity for branched aldehyde under catalytic conditions. Interestingly, we also find that acyl dicarbonyl complexes **7b**$_{va}$ and **7b′**$_{va}$ are formed even in the presence of H_2 and persist for hours under an atmosphere of syngas with passive mixing at −10 °C. For the unobserved acyl monocarbonyl intermediates produced by insertion of coordinated CO into the branched Rh-alkyl, there is competition between CO coordination, reaction with dihydrogen, and isomerization. Evidently the oxidative addition of H_2 (and subsequent reductive elimination of the product) is not competitive with CO association under these conditions of low temperature and low concentration of dissolved dihydrogen.

Some isomerization of the branched acyls to linear acyl "7l$_{va}$" occurs slowly over the course of the reaction; however, the branched isomers predominate by a ratio of 2.6:1 after about 4 h, a time at which equilibrium has not been achieved.

For vinyl acetate, the ratio of the diastereomeric acyl complexes reveals a slight kinetic preference (1.2:1) for **7b**$_{va}$ which is eventually overtaken by a slight thermodynamic preference (1.1:1) for **7b′**$_{va}$. These small countervailing preferences are consistent with the low enantioselectivity of this system. This equilibration between acyl complexes, along with continuing isomerization to the linear isomer, indicates that all steps leading to the formation of the acyl complexes are reversible under these conditions.

Characterization of Alkyl Complexes. The $^{31}P\{^{1}H\}$ NMR spectrum shows at least five additional species, in addition to [Rh(acac)(BDP)] and a rhodium dimer. Three of these can be tentatively identified as alkyl complexes, as indicated by the absence of any additional signals in the acyl region of the ^{13}C NMR spectrum (Chart 2). Identification of alkyl intermediates along the hydroformylation catalytic cycle is rare.

Chart 2. Alkyl Complexes Formed Following the Reaction of 1 with Vinyl Acetate

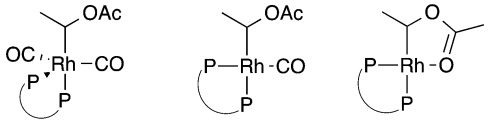

The species we have assigned as **4b**$_{va}$ has phosphorus signals at δ 82.6 and 39.2 ppm, and shows one new 89 Hz $^{31}P-^{13}C$ splitting (in the upfield peak) following the reaction of vinyl acetate with [Rh(H)(^{13}CO)$_2$(BDP)]; along with its two large $^{1}J_{PRh}$ values (101 and 213 Hz), this suggests it is a four-coordinate alkyl complex. (Note: this designation should not be taken to imply that **4b**$_{va}$ and **7b**$_{va}$ have the same absolute stereochemistry; we are not currently able to determine the configuration of any of these species.) $^{1}H-^{31}P$ HMBC shows correlation of the upfield P resonance to an apparent triplet at δ

DOI: 10.1021/jacs.5b09858
J. Am. Chem. Soc. 2015, 137, 14208−14219

1.58 ppm in the ^{1}H NMR spectrum, which shows through-bond coupling to a multiplet at δ 4.69 ppm. We propose that the upfield signal is actually a doublet of doublets belonging to a methyl group; the second 6.5 Hz coupling is created by the trans ligand phosphorus atom. While a triplet might seem to be more consistent with the methyl group of an ethyl fragment, the ^{1}H−^{1}H COSY correlation to a single downfield signal belies this simple assignment: methylene protons would almost certainly be further upfield. Moreover, in all other linear [Rh(BDP)] complexes characterized thus far, the diastereotopic methylene protons have had a substantial (ca. 1 ppm) difference in chemical shift. Therefore, we ascribe these signals to branched alkyl **4b$_{va}$**. The signal from the methine proton at about δ 4.69 ppm is not observable in the simple 1D spectrum, although it is clearly observed in the 2D COSY and ^{1}H−^{31}P HMBC spectra. However, because this signal would be at least a doublet of quartets (and possibly a ddq) in a crowded region of the spectrum, the absence of a clear peak for the methine proton in the simple 1D NMR spectrum is not surprising.

Five-coordinate branched alkyl complex **5b$_{va}$** was identified by its moderate (83 and 159 Hz) phosphorus−rhodium coupling constants, the presence of two CO ligands (both cis to the ligand's phosphorus atoms, as established by labeling with ^{13}CO), and through-bond coupling to, as above, an apparent triplet at δ 1.4 ppm in the ^{1}H NMR spectrum showing through-bond coupling to a downfield (δ 4.7 ppm) signal. In the ^{31}P NMR spectrum (see Figure 4), another small set of doublets-

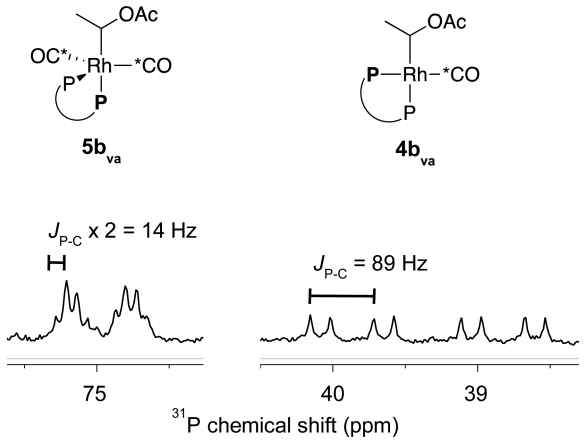

Figure 4. Partial ^{31}P{^{1}H} NMR spectrum taken following the reaction of [Rh(H)(^{13}CO)$_2$(BDP)] with vinyl acetate. Ligand phosphorus atoms show two new $^{2}J_{PC}$ for **5b$_{va}$** (left) and one for **4b$_{va}$** (right). Labeled carbons are denoted by "*" (202.5 MHz, −40 °C, CD_2Cl_2).

of-doublets appears just upfield of each ^{31}P signal for **5b$_{va}$**. The signals are too small to provide any useful characterization information, but because of the similarity of their spectral features to those of **5b$_{va}$**, they could plausibly belong to the other diastereomer, **5b′$_{va}$**. If that is the case, the diastereomeric ratio for these alkyl complexes is 3.9:1—much greater than that observed at the acyl stage.

The final alkyl species has no CO ligands, which, along with its large (256 and 129 Hz) $^{1}J_{PRh}$ and apparent correlation to a broad quartet in the ^{1}H NMR spectrum leads us to assign it as **4b*$_{va}$**, in which the acetate group occupies the fourth coordination site. In the absence of additional characterization data this assignment is speculative because there is no spectroscopic indication of carbonyl coordination. The regiochemistry of this species is clearly branched, and the coupling data are indicative of a square planar or perhaps T-shaped complex.

There is a fourth, unidentified species, with broad phosphorus signals at δ 78.5 and 54.6 ppm. Its large (107 and 221 Hz) phosphorus−rhodium coupling constants suggest that it is a four-coordinate species (although the peaks are too broad following labeling with ^{13}CO to provide any more-conclusive information). Through-bond coupling to a quartet and doublet in the ^{1}H NMR spectrum are consistent with a branched species. These peaks tentatively are assigned to four-coordinate branched acyl **6b$_{va}$**. For NMR data for alkyl and acyl complexes generated from the reaction of **1** with vinyl acetate, see Table S1.

Proposal for the Formation of "7l$_{va}$". Propionyl complex "**7l$_{va}$**" could plausibly be formed by the reaction of hydride **1** (or monocarbonyl hydride **2**, not observed) with ethene. We propose that the unseen linear alkyl intermediate **4l$_{va}$** is formed from the isomerization of the kinetically favored branched alkyl complexes. **4l$_{va}$** undergoes β-acetoxy elimination to form ethene, which subsequently dissociates and goes on to react with another rhodium hydride to generate "**7l$_{va}$**" (see Scheme 3). (Even after dicarbonyl hydride **1** has been consumed, the

Scheme 3. Proposal for the Formation of Propionyl Complex 7l$_{va}$

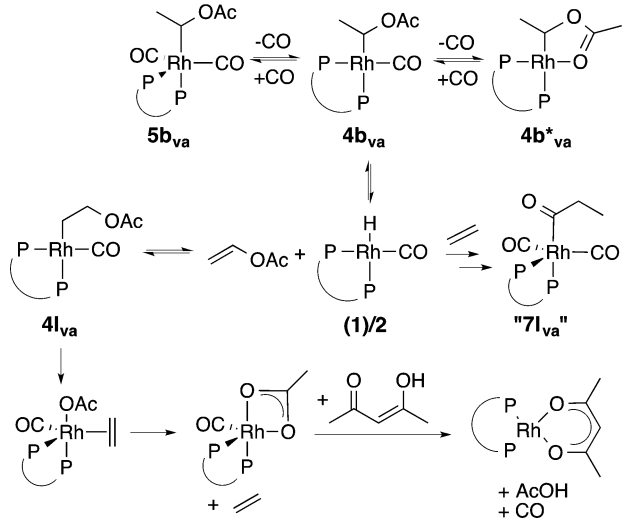

equilibration of alkyl and acyl complexes implies that **2** persists in solution, albeit below the limit of detection.) The β-acetoxy elimination reaction is commonly cited in transition metal mediated reactions, although most commonly for group 10 metals;[17] however, it has been specifically invoked to explain the reaction of a variety of metal hydrides (including rhodium) with vinyl acetate to generate ethylene.[18] Also, our group has reported observation of β-elimination of trifluoroacetoxy groups (a better leaving group than acetate) during the AHF of enol trifluoroacetate esters.[18c]

β-acetoxy elimination from **4l$_{va}$** yields a rhodium acetate complex as well as ethene (see Scheme 3). We hypothesize that the reaction of ethene with **2** is fast because no free ethene is observed in the ^{1}H NMR spectrum. We do not see any evidence for a rhodium acetate species; however, we do see [Rh(acac)(BDP)] build up at a rate that is identical to the rate of formation of "**7l$_{va}$**" (Figure 3). This could suggest that any

DOI: 10.1021/jacs.5b09858
J. Am. Chem. Soc. 2015, 137, 14208−14219

Rh-acetate intermediate undergoes fast exchange with acetylacetone which is present from the initial generation of the [RhH(CO)$_2$(BDP)] (Scheme 3). Thus, the loss of branched alkyl complexes, **4b$_{va}$**, **5b$_{va}$**, and **4b$_{va}$**, is replaced by a 1:1 mixture of [Rh(acac)(BDP)] and "**7l$_{va}$**". This interpretation of the data is speculative but reasonable; control experiments establish that *in situ* generated [Rh(OAc)(BDP)] and acetyl acetone react to form [Rh(acac)(BDP)] (see Supporting Information).

The high selectivity for the branched product in catalytic hydroformylation of vinyl acetate seems to be reflected in the strong kinetic preference for branched alkyl and acyl complexes versus their linear counterparts. In fact, the only linear species observed is propionyl acyl complex "**7l$_{va}$**", and this species is presumably formed from ethylene addition to the hydride **2** (which produces degenerate insertion products).

Allyl Cyanide. Addition of allyl cyanide to a solution of **1** at −10 °C under an atmosphere of CO gives the five-coordinate linear acyl complex **7l$_{ac}$** as the major product (regiochemistry determined by ^{1}H−^{31}P HMBC spectroscopy). The apparent half-life for the disappearance of **1** in this experiment is approximately 4 min (see Supporting Information). The reaction timecourse at −20 °C is shown in Figure 5. Colder

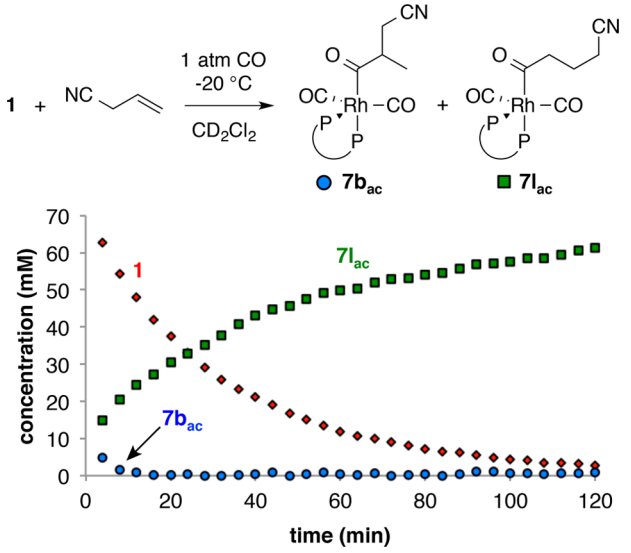

Figure 5. Reaction of **1** (red diamonds) with allyl cyanide gives predominantly linear acyl **7l$_{ac}$** (−20 °C, 15 psia CO, 90 mM **1**, 400 mM allyl cyanide, CH_2Cl_2).

temperatures were used to see the branched acyl dicarbonyl species. The remaining mass balance comprises uncharacterized complexes in low concentrations (see Supporting Information). The coordination number of **7l$_{ac}$** was determined by labeling with ^{13}CO as described above.

While the minor species produced by this reaction proved difficult to characterize definitively, the most promising candidate for branched acyl **7b$_{ac}$** based on chemical shift and coupling constants is the set of two doublets-of-doublets at δ 68.6 ppm ($^1J_{PRh}$ = 80 Hz, $^2J_{PP}$ = 17 Hz) and δ 59.7 ppm ($^1J_{PRh}$ = 169 Hz, $^2J_{PP}$ = 17 Hz). The apparent thermodynamic instability of this species, which is already decreasing in concentration when the first spectrum is recorded (see Figure 5), is consistent with this assignment, since we expect allyl cyanide to exhibit the typical steric preference for the linear acyl. An obstacle to characterizing these species concerns the difficulty of synthesizing of the ^{13}C-labeled substrate.

***trans*-1-Phenyl-1,3-butadiene.** The reaction of *trans*-1-phenyl-1,3-butadiene with **1** at 0 °C under an atmosphere of CO gives five-coordinate acyl complexes and an allyl complex as the major products (Figure 6). The diastereomeric acyl

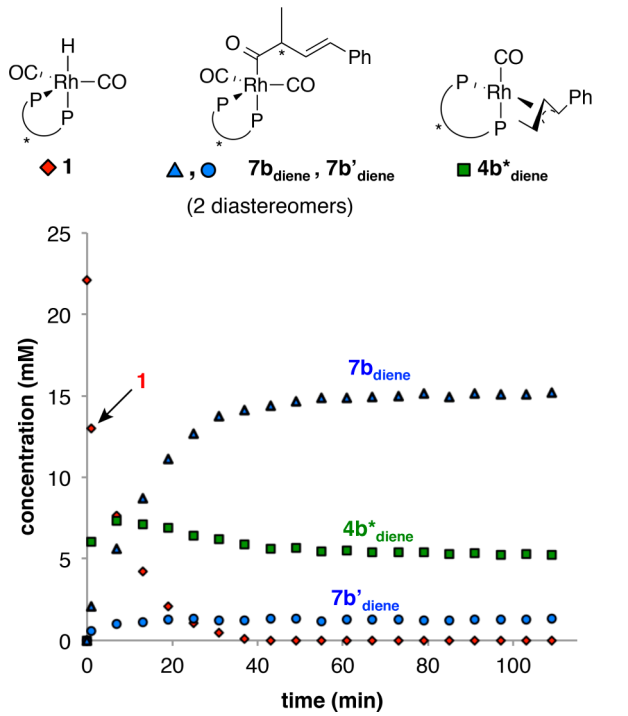

Figure 6. Reaction of **1** (red diamonds) with *trans*-1-phenyl-1,3-butadiene leads to primarily the 2-formyl acyl **7b$_{diene}$** and the allyl species **4b*$_{diene}$** (0 °C, 15 psia CO, 22 mM **1**, 200 mM *trans*-1-phenyl-1,3-butadiene, CH_2Cl_2). For plot highlighting mass balance, see Supporting Information.

complexes **7b$_{diene}$** and **7b′$_{diene}$** are responsible for the eight-line patterns at δ 68.9, 60.8 ppm and δ 67.0, 59.1 ppm, respectively, in the ^{31}P{^{1}H} NMR spectrum. The allyl complex, **4b*$_{diene}$**, appears as a four-line pattern at δ 78.3 and 48.1 ppm. At −10 °C, the qualitative half-life for the disappearance of **1** is 20 min (see Supporting Information).

Characterization of Acyl Complexes. As with the other substrates, the regiochemistry of acyl complexes formed from *trans*-1-phenyl-1,3-butadiene was determined using ^{1}H−^{31}P HMBC spectroscopy. The ligand phosphorus atoms show long-range coupling to methine protons for both observed acyl complexes. Selective 1D-TOCSY spectra with irradiation at these proton peaks elucidated the regiochemistry. Other two-dimensional NMR spectra, including ^{31}P−^{31}P COSY and ^{1}H−^{13}C HSQC, are consistent with these assignments.

The characterization of these species as acyl, rather than alkyl, complexes was made using ^{1}H−^{13}C HSQC spectroscopy. The methine protons of **7b$_{diene}$** and **7b′$_{diene}$** were correlated to carbon atoms at δ 70.8 ppm. In the branched styrenyl acyl complex **7b$_{sty}$**, the methine carbon appears at δ 74.0 ppm versus δ 37.7 ppm for the alkyl species.[11]

The coordination number for these complexes was determined by labeling with ^{13}CO. For **7b$_{diene}$** the axial phosphorus resonance is an apparent triplet of quartets with another multiplet underneath obscuring the structure slightly; *J*

DOI: 10.1021/jacs.5b09858
J. Am. Chem. Soc. 2015, 137, 14208−14219

= 81.8, 15.9 Hz (Figure 7). This multiplet is correctly interpreted as a dddt, but one $^2J_{PC}$ happens to be equal to

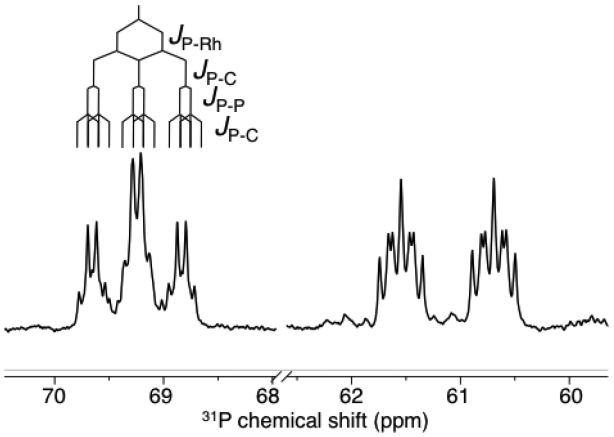

Figure 7. $^{31}P\{^1H\}$ NMR spectrum demonstrating the use of ^{13}C labeling to determine the coordination number of $\mathbf{7b}_{diene}$. The multiplet is an apparent triplet of quartets (0 °C, 15 psia ^{13}CO, 30 mM **1**, 260 mM *trans*-1-phenyl-1,3-butadiene, CH_2Cl_2).

the $^1J_{PRh}$ coupling constant, and the other two $^2J_{PC}$ are equal to the $^2J_{PP}$ value. The downfield multiplet for $\mathbf{7b'}_{diene}$ appears to have a similar structure; however, its relatively low concentration prevents exact determination of coupling constants.

Characterization of Allyl Complex $\mathbf{4b*}_{diene}$. The regiochemistry of the allyl species was determined by $^1H-^{31}P$ HMBC and selective 1D-TOCSY experiments. The proton peaks appear at δ 1.57, 1.72, 3.82, and 5.34 ppm, which are consistent with other reported Rh-allyl complexes.[9,19] DEPT

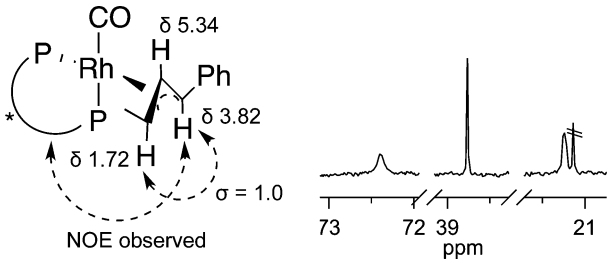

Figure 8. ^1H NMR assignments of allyl protons and observed NOE between anti protons and the ligand (left). ^{13}C NMR spectrum of allyl carbon peaks in $\mathbf{4b*}_{diene}$ (right) (0 °C, 15 psia CO, 22 mM **1**, 200 mM *trans*-1-phenyl-1,3-butadiene, CH_2Cl_2).

experiments assisted in the assignments shown in Figure 8. $^1H-^{13}C$ HMBC spectroscopy support the presence of an allyl species by the lack of an acyl carbon peak; the proton signal at δ 3.82 ppm showed no ^{13}C cross peaks above δ 150 ppm in the $^1H-^{13}C$ HMBC spectrum.

The coordination number of $\mathbf{4b*}_{diene}$ was determined by labeling with ^{13}CO. Both of the ^{31}P signals for $\mathbf{4b*}_{diene}$ show one additional coupling in the reaction with *trans*-1-phenyl-1,3-butadiene and $Rh(H)(^{13}CO)_2(BDP)$. The phosphorus atom trans to CO has $^2J_{PC}$ = 38.0 Hz, and cis gives $^2J_{PC}$ = 10.3 Hz.

Selective 1D-NOESY experiments were used to determine the syn/anti relationship of the substituents. When the peak at δ 3.82 ppm was irradiated, an NOE was observed with the proton that appears at δ 1.72 ppm with an initial build-up rate of σ = 1.0 s^{-1}. The lack of NOE to the proton resonating at 5.34 ppm and the significant NOE between the protons resonating at 1.72 and 3.82 ppm provides evidence for the structure shown in Figure 8.

We have assigned this complex as an η^3-allyl, but an η^1 complex also was considered. $^1H-^{13}C$ HSQC spectroscopy was used to identify the ^{13}C NMR signals for the allyl ligand. In the $^{13}C\{^1H\}$ NMR spectrum, these peaks are broad multiplets; while the peaks' low intensity prevents exact determination of coupling constants, their shape suggests an η^3-allyl species with $^1J_{CRh}$ and $^2J_{CP}$ coupling.

1-Octene. Because 1-octene undergoes AHF to give predominantly linear product, stoichiometric NMR studies of this substrate provides an instructive counterpoint to results obtained with styrene and other more electron-deficient substrates.

It is also important to point out that, unlike styrene, 1-octene can isomerize under hydroformylation conditions to give internal alkenes, primarily 2-octene (in hydroformylation with the methylbenzylamide BDP ligand, at 50 °C and 150 psig H_2/CO, 32% of the starting material had isomerized to 2-octene after 24 h).[15] Therefore, alkyl and acyl complexes derived from the reaction of **1** with internal alkenes should be considered as possible products.

As with the other substrates, the major product of the reaction of 1-octene with **1** is a five-coordinate dicarbonyl acyl complex. At −10 °C, the half-life for the disappearance of hydride is approximately 3 min (see Supporting Information). The reaction was monitored at lower temperatures to better observe the kinetic selectivity early in the reaction. At −20 °C in the absence of H_2, the linear acyl $\mathbf{7l}_{oct}$ product dominates (Figure 9), as seen for styrene and allyl cyanide. The branched acyl $\mathbf{7b}_{oct}$ could only be observed when the reaction temperature was lowered to −30 °C to monitor speciation very early in the reaction. Again, the regiochemistry of $\mathbf{7l}_{oct}$ was determined by $^1H-^{31}P$ HMBC (see Supporting Information). The concentration of $\mathbf{7b}_{oct}$ was too low to give a cross peak in the 2D spectrum; however, the observation of a doublet in the ^1H NMR spectrum early in the reaction at δ 0.37 ppm, and comparison of the chemical shifts and coupling constants in the ^{31}P NMR spectrum, corroborate this assignment.

The minor species were more difficult to characterize and quantify, leading to a slight loss of mass balance (ca. 5−10%). Most minor species were not well-resolved until the temperature was lowered to −40 or −80 °C. The two most prominent minor species have eight-line patterns at δ 70.8 and 67.4 ppm and δ 63.2 and 57.6 ppm. We have tentatively characterized these as $\mathbf{5b}_{oct}$ and $\mathbf{4b}_{oct}$, respectively (see Chart 3). Generating these species with 1-^{13}C-octene demonstrates that neither is a linear isomer (insertion at the 1-position of the alkene would result in measurable $^{31}P-^{13}C$ coupling for both alkyl and acyl species). However, it is important to point out that, while these species have been drawn with methyl branches, the data from this ^{13}C-labeling experiment are also consistent with complexes formed by the insertion of internal octenes, the products of alkene isomerization, into the R−H bond of **1**. We do not currently have any data that would rule out species of this type. Indeed, the presence of at least two distinct types of ^{13}C-labeled methyl groups in the ^1H and ^{13}C NMR spectra shows that isomerization is occurring under these conditions. (Of course, isomerization must also occur during the reaction of **1** with unlabeled substrate; however, the crowded alkyl and vinyl

DOI: 10.1021/jacs.5b09858
J. Am. Chem. Soc. 2015, 137, 14208−14219

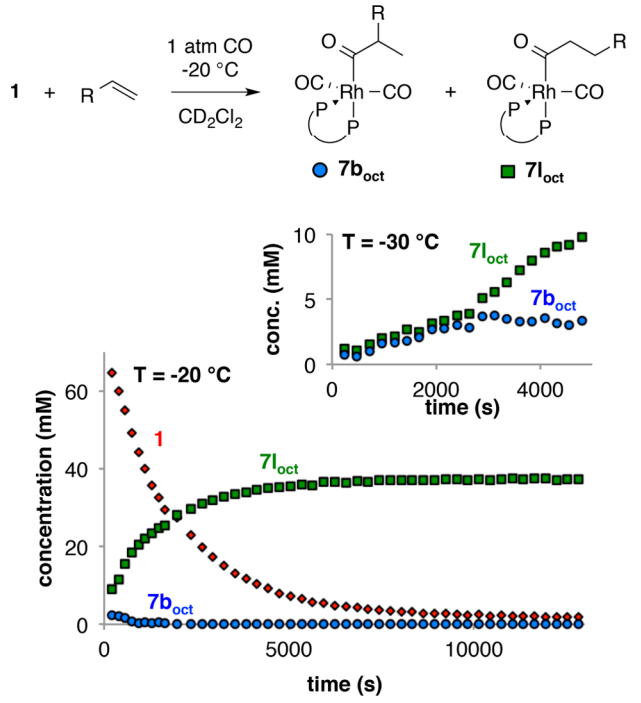

Figure 9. Plots demonstrating apparent kinetic b:l selectivity for 1-octene can be resolved at −30 but not −20 °C under passive mixing conditions. Reaction of **1** (red diamonds) with 1-octene gives predominantly linear acyl $\mathbf{7l}_{oct}$ (−20 °C, 15 psia CO, 80 mM **1**, 400 mM 1-octene, CH_2Cl_2). Spectra taken at lower temperature and short reaction times (inset) show no kinetic preference for either regioisomer, in contrast with the results for styrene (−30 °C, 15 psia CO, 65 mM **1**, 320 mM 1-octene, CH_2Cl_2). R = C_6H_{13}.

Chart 3. Alkyl Species Tentatively Characterized Following the Reaction of 1 with 1-Octene

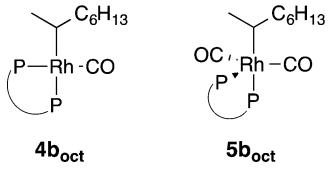

$\mathbf{4b}_{oct}$ $\mathbf{5b}_{oct}$

regions of these spectra make detection of isomerization virtually impossible without isotopic enrichment.)

The NMR spectrum of $\mathbf{5b}_{oct}$ taken after addition of 1-octene to ^{13}CO-labeled [Rh(H)(^{13}CO)$_2$(BDP)] shows two new poorly resolved ^{31}P−^{13}C couplings, consistent with an alkyl dicarbonyl, where the phosphorus atom (P_{eq}) showing the new coupling shares the equatorial plane with the two labeled carbon atoms. Complex $\mathbf{4b}_{oct}$, on the other hand, shows one new 34 Hz phosphorus−carbon splitting to the upfield phosphorus signal (P_{ax}), while the downfield peak (P_{eq}) shows a larger 81 Hz coupling. These data are consistent with an alkyl monocarbonyl structure for which the large coupling belongs to the phosphorus atom *trans* to the labeled carbonyl group. Curiously, for the other alkyl complexes identified the phosphorus atom that is positioned *trans* to the organic fragment is responsible for the downfield signal. If the structural assignment of $\mathbf{4b}_{oct}$ is correct, the downfield signal belongs instead to the phosphorus atom *trans* to the carbonyl ligand. We do not currently have any explanation for this change in upfield versus downfield shift trends; however, the difference in magnitude of the phosphorus−carbon coupling constants would make a different assignment of the coordination geometry implausible.

Unfortunately, the absence of strong correlations in the ^{1}H−^{31}P HMBC spectrum prevents the use of ^{1}H NMR data to further substantiate these assignments. The ^{13}C NMR spectra of the material generated using either ^{13}CO or 1-^{13}C-octene are similarly unhelpful; however, the acyl region of the former seems to have at least two minor acyl signals in the baseline (in addition to the major peak for $\mathbf{7l}_{oct}$), suggesting that at least one of the unresolved species in the baseline may be another acyl complex. See Table S1 for NMR data for $\mathbf{7b}_{oct}$, $\mathbf{7l}_{oct}$, $\mathbf{4b}_{oct}$, and $\mathbf{5b}_{oct}$.

At equilibrium, rhodium complex speciation in the non-catalytic reaction of **1** with 1-octene resembles, in general terms, that seen with styrene: the five-coordinate linear acyl dominates, accounting for more than 50% of the total ^{31}P integration. However, the data early in the reaction, under conditions where $\mathbf{7b}_{oct}$ is observable, reveal an important distinction. Whereas for styrene there was a clear kinetic preference for the branched acyl $\mathbf{7b}_{sty}$ (presumably reflecting a preference for the branched intermediate $\mathbf{4b}_{sty}$), 1-octene displays no such preference (see Figure 12). The two species grow in at roughly the same rate.

If we assume that the kinetic behavior of the acyl species reflects the kinetic behavior of the alkyl species, and that the relative rates of alkene insertion to give alkyl complexes **4** is the primary factor governing selectivity, the results presented in Figure 12 are consistent with the experimental observation of low selectivity in 1-octene hydroformylation by Rh(BDP) catalysts.

NMR Studies at Higher Pressure with Active Mixing. *Equilibration of the Allyl Complex* $\mathbf{4b*}_{diene}$ *and the Acyl Dicarbonyl* $\mathbf{7b}_{diene}$. A limitation of low-pressure studies with passive mixing is that the concentration of CO in solution is unknown and not controlled during the reaction.[19] Our group has recently reported the development of the Wisconsin high-pressure NMR reactor (WiHP-NMRR). The apparatus allows for the collection of data under a known pressure with active gas−liquid mixing.[20]

The reaction of **1** with *trans*-1-phenyl-1,3-butadiene at 0 °C was monitored under a constant pressure of 5 psig CO with active mixing (Figure 10). The WiHP-NMRR experiment shows a higher concentration of $\mathbf{4b*}_{diene}$ than in the low-pressure studies—we attribute this to the uncertain and inconstant [CO] in the passively mixed low-pressure experiments. As expected, as the pressure of CO (and consequently, the dissolved CO concentration) increases, the equilibrium favors $\mathbf{7b}_{diene}$ (see Supporting Information). The lower sensitivity of the 360 MHz spectrometer used for WiHP-NMRR studies yields noisier ^{31}P NMR spectra than the other examples reported herein, and thus, the diastereomer, $\mathbf{7b'}_{diene}$ was below the detection limit under these conditions.

After the reaction of the diene and [Rh(H)(BDP)(CO)$_2$] reached equilibrium, the CO pressure was increased and the changes in the [$\mathbf{7b}_{diene}$]/[$\mathbf{4b*}_{diene}$] ratio were observed. From these data the equilibrium constant for reaction 2 (Figure 11), K_{eq}, was determined (see Supporting Information). The equilibrium expression was rearranged such that plotting [CO]^2 versus [$\mathbf{7b}_{diene}$]/[$\mathbf{4b*}_{diene}$] gives a line with a slope of $K_{eq} = k_2/k_{-2} = 6973$.

Simplified reactions were entered into the kinetic modeling program COPASI for determination of rate constants for the formation of $\mathbf{4b*}_{diene}$ and $\mathbf{7b}_{diene}$.[21] The rate constants for k_1,

DOI: 10.1021/jacs.5b09858
J. Am. Chem. Soc. 2015, 137, 14208−14219

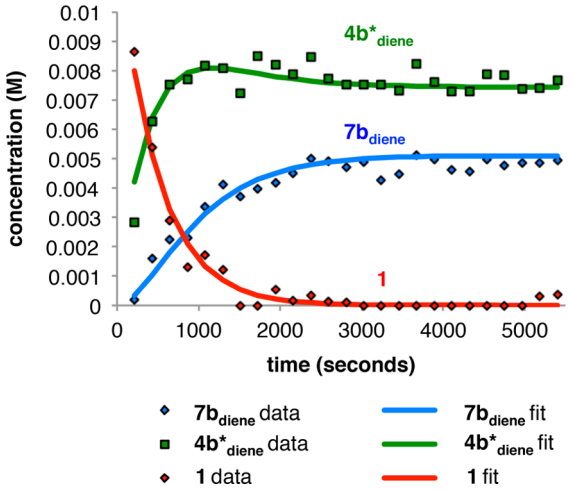

Figure 10. Reaction of **1** (13 mM) with *trans*-1-phenyl-1,3-butadiene (61 mM) at 0 °C under a constant pressure of 20 psia as measured by WiHP-NMRR. The data were modeled in COPASI.

Reaction 1

a) **1** + *trans*-1-phenyl-1,3-budadiene $\xrightarrow{k_1}$ **4b***$_{diene}$ + CO

Reaction 2

4b*$_{diene}$ + 2 CO $\underset{k_{-2}}{\overset{k_2}{\rightleftharpoons}}$ **7b**$_{diene}$

b)

	Value	Standard Deviation
k_1	2.09x10^{-3} M^{-1}s^{-1}	5x10^{-5}
k_2	7.4 M^{-2} s^{-1}	7x10^{-1}
k_{-2}	1.1x10^{-3} s^{-1}	1x10^{-4}

Figure 11. (a) Simplified kinetic model for determination of rate constants of formation of products of the reaction of **1** and *trans*-1-phenyl-1,3-butadiene at 0 °C in the absence of H_2 and approximately 17 psia CO and (b) rate constants and standard deviations estimated by nonlinear least-squares fitting.

k_{-1}, and k_2 were calculated by fitting the data; k_{-2} was set based on k_2 and the known value for K_{eq} (Figure 11). The data were fit best when a pressure of CO of 17 psia was entered into the model (Figure 8). The pressure transducer used has an accuracy of ±3 psi; thus, 17 psia falls within this range. See Supporting Information for other plots.

These calculations show that the rate of formation of the allyl complex (k_1) is significantly smaller than its trapping by CO (k_2[CO]) to form an acyl dicarbonyl complex. A rate constant (k_{-1}, not shown) for deinsertion of the allyl complex to form **1** and *trans*-1-phenyl-1,3-butadiene was optimized, but found to be insignificantly small; therefore, this step was modeled as irreversible. The calculated equilibrium constant indicates that, under the higher CO pressures used in standard hydroformylation reactions, the acyl dicarbonyl species is favored thermodynamically over the allyl complex. However, this equilibrium distribution may not be realized under catalytic conditions because dihydrogen may competitively trap the acyl monocarbonyl intermediate to ultimately yield **1** plus aldehyde.

The WiHP-NMRR apparatus enables analysis of the kinetics and thermodynamics of the equilibration of **1**, **4b***$_{diene}$, and **7b**$_{diene}$ not previously attainable. Under increasingly high pressures of CO, the equilibrium is shifted toward the acyl dicarbonyl complex. In contrast with our previous studies, use of WiHP-NMRR assures that the CO partial pressure is known and that the equilibrium concentration of dissolved CO (i.e., Henry's law equilibrium) is rigorously maintained throughout the reaction.

Selectivity of Acyl Formation and Hydrogenolysis for Allyl Cyanide. At temperatures <0 °C and 1 atm of passively mixed CO, reaction of **1** with allyl cyanide proceeds with a half-life of a few minutes, thermodynamics clearly favor linear acyl dicarbonyl **7l**$_{ac}$, and the kinetic selectivity seems to slightly favor the branched acyl. What happens if the reaction is performed with active CO mixing?

As shown in Figure 12, reaction of hydrido dicarbonyl with one equivalent of allyl cyanide at 17 psia CO at 0 °C in the

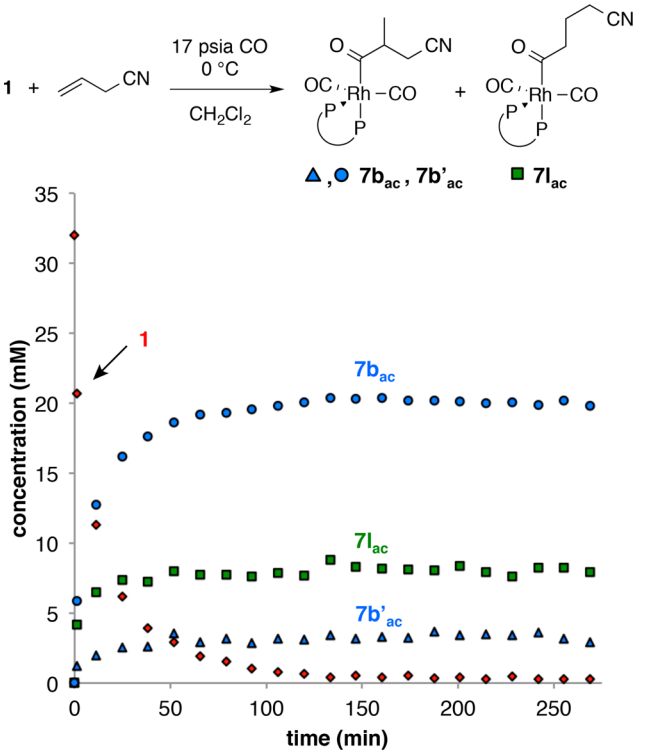

Figure 12. Reaction of **1** (32 mM) with allyl cyanide (32 mM) at 0 °C under a constant pressure of 17 psia CO as measured by WiHP-NMRR with active mixing.

presence of active gas mixing yields a distinct kinetic preference for the formation of one diastereomer **7b**$_{ac}$ of the *branched* acyl dicarbonyl with an overall branched:linear ratio of about 3:1; the two branched diastereomers are distinguishable and appear in a ratio of about 5:1.[22] With active mixing at 0 °C these ratios are maintained for 3 h with little change. However, warming the solution to room temperature with active mixing initiates isomerization of the branched acyls to the linear (see Supporting Information). Isomerization can be effectively stopped by cooling back to 0 °C. These data conclusively demonstrate that (a) the branched acyl dicarbonyls are the kinetic products, (b) the linear acyl dicarbonyl **7l**$_a$ is the thermodynamic product, (c) the rate of isomerization is inhibited by CO, and (d) the reaction of **1** with allyl cyanide is inhibited by CO.

What about selectivity in the presence of H_2? By creating a nonequilibrium ratio of linear and branched acyl dicarbonyls at about 1:1 and then adding H_2 with active mixing we can

DOI: 10.1021/jacs.5b09858
J. Am. Chem. Soc. 2015, 137, 14208–14219

directly examine the relative hydrogenolysis rates of linear and branched acyl dicarbonyls. The results are shown in Figure 13.

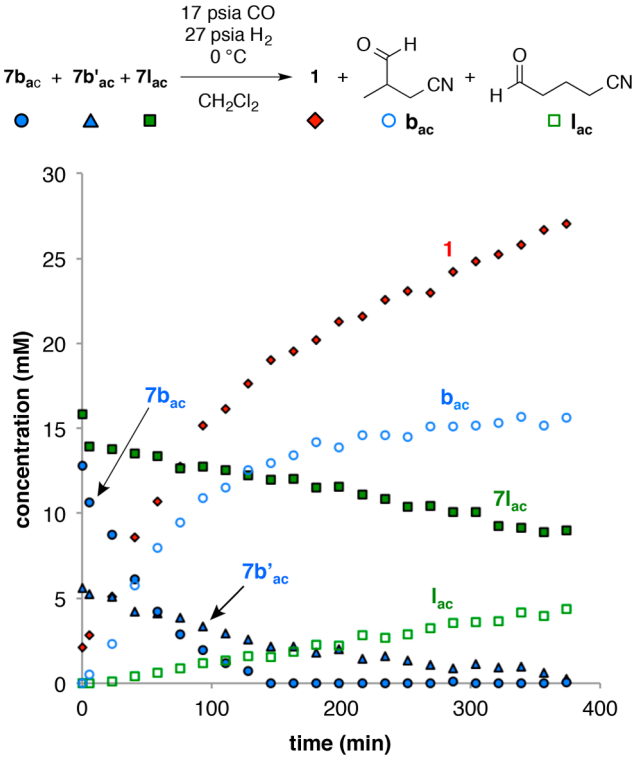

Figure 13. Hydrogenolysis of a nonequilibrium distribution of acyl dicarbonyl species ($7l_{ac}$, $7b_{ac}$, $7b'_{ac}$) (32 mM, b:l ~ 1) to produce linear (l_a) and branched (b_a) aldehydes at 0 °C under a constant pressure of 17 psia CO and 27 psia H_2 as measured by WiHP-NMRR with active mixing.

Starting from near equal amounts of linear and branched acyl dicarbonyls, branched aldehyde clearly forms faster than linear. Furthermore, the data demonstrate that little isomerization of linear and branched acyls occurs over the 5 h reaction time (as seen in the absence of H_2, *vide supra*). Hydrogenolysis rates differ significantly for the two branched diastereomers with $7b_a$ disappearing 3-fold faster than $7b'_a$. Such reactions with dihydrogen demonstrate substantial intrinsic selectivities for hydrogenolysis of acyl dicarbonyls and that, at these temperatures and pressures, the rate of hydrogenolysis is faster than equilibration among the various acyl dicarbonyls (non-Curtin–Hammett conditions). These results indicate the power of single-turnover experiments in the WiHP-NMRR for elucidating the detailed kinetics of acyl formation and hydrogenolysis in hydroformylation.

CONCLUSIONS

One motivation of these studies is determination of the spectroscopic signatures of alkyl, acyl, and allylic intermediates relevant to AHF for a representative sampling of different substrate types. Such data are essential to establish the relative rates and thermodynamic stabilities of catalyst intermediates that constitute the "inside-out" mechanistic approach. These studies have been facilitated by adopting low-temperature and low-pressure reaction conditions without H_2 present and passive gas–liquid mixing. Many catalytic intermediates have been intercepted and characterized by detailed NMR studies. These intermediates include the rarely observed alkyl and acyl monocarbonyl intermediates of catalytically active complexes.

The data reported herein indicate that, at low temperatures, modest CO pressures, and without H_2 present, acyl dicarbonyl complexes form rapidly and with thermodynamic preference over the intermediary alkyl and acyl monocarbonyl complexes. Indeed, alkyl and acyl monocarbonyl complexes only appear under conditions where dissolved CO becomes almost completely depleted. The notable exception occurs with *trans*-1-phenyl-1,3-butadiene as the substrate; intramolecular η^3-coordination competes with bimolecular CO association in this case. The data compellingly demonstrate that, for simple α-olefins (styrene, octene, allyl cyanide), thermodynamics prefer linear acyl dicarbonyls over branched, but that kinetics generally favor the branched isomers. With vinyl acetate and *trans*-1-phenyl-1,3-butadiene analysis is complicated by β-acetoxy elimination and by formation of stable η^3-allyls, respectively.

High-pressure NMR equipment, such as the WiHP-NMRR, enables informative examination of acyl formation and hydrogenolysis under actively mixed conditions. For *trans*-1-phenyl-1,3-butadiene, the kinetics of equilibration between η^3-allyl and acyl dicarbonyls are probed directly. More significantly, single-turnover experiments involving actively mixed gases at superambient pressures enable the selectivity of acyl dicarbonyl formation and hydrogenolysis steps to be probed independently. For allyl cyanide the data demonstrate that the kinetically favored branched acyl dicarbonyl diastereomer also reacts faster with H_2 than either the more slowly formed branched diastereomer or the linear diastereomer.

The significance of this work is threefold. First, it represents the broadest effort so far to characterize catalyst intermediates that are relevant to one of the largest industrial applications of homogeneous, organotransition metal catalysis. Second, the data provide strong evidence that the kinetics and selectivities of formation of off-cycle acyl dicarbonyl isomers under low-temperature, noncatalytic conditions reflect the general catalytic selectivities at higher temperatures. Finally, single-turnover experiments performed at superambient pressures with active gas–liquid mixing and NMR detection constitute a powerful divide-and-conquer strategy to understanding the origins of catalytic activity and selectivity in hydroformylation. Such studies will be the subject of future publications.

We also note that the conclusions and observations drawn from this study are specific to the BDP-ligated catalyst. It is well-known that the catalytic properties are strongly influenced by the ligand structure. Thus, the generality of the results reported is not yet known.

ASSOCIATED CONTENT

Supporting Information

The Supporting Information is available free of charge on the ACS Publications website at DOI: 10.1021/jacs.5b09858.

Experimental procedures, selected NMR spectra, and modeling data (PDF)

AUTHOR INFORMATION

Corresponding Author

*landis@chem.wisc.edu

Present Address

†E.R.N.: Institute for Critical Technology and Applied Science, Virginia Tech, Blacksburg, Virginia.

DOI: 10.1021/jacs.5b09858
J. Am. Chem. Soc. 2015, 137, 14208–14219

Author Contributions

‡E.R.N. and A.C.B. contributed equally.

Notes

The authors declare no competing financial interest.

■ ACKNOWLEDGMENTS

The authors thank Dr. Charlie Fry for generous assistance with NMR experiments, Professor Charles P. Casey for helpful discussions, and the NSF for funding (DGE-1256259 and CHE-1152989).

■ REFERENCES

(1) For reviews of hydroformylation, see (a) Agbossou, F.; Carpentier, J.-F.; Mortreux, A. *Chem. Rev.* **1995**, *95*, 2485−2506. (b) Claver, C.; van Leeuwen, P. W. N. M. In *Rhodium Catalyzed Hydroformylation*; Claver, C., van Leeuwen, P. W. N. M., Eds.; Kluwer Academic Publishers: Dordrecht, The Netherlands, 2000. (c) Wiese, K.-D.; Obst, D. *Top. Organomet. Chem.* **2006**, *18*, 1−33. (d) Franke, R.; Selent, D.; Börner, A. *Chem. Rev.* **2012**, *112*, 5675−5732.

(2) Botteghi, C.; Paganelli, S.; Schionato, A.; Marchetti, M. *Chirality* **1991**, *3*, 355−369.

(3) For examples of catalysts for asymmetric hydroformylation, see: (a) Wink, J. D.; Kwok, T. J.; Yee, A. *Inorg. Chem.* **1990**, *29*, 5006−5008. (b) Gladiali, S.; Pinna, L. *Tetrahedron: Asymmetry* **1991**, *2*, 623−632. (c) Sakai, N.; Nozaki, K.; Mashima, K.; Takaya, H. *Tetrahedron: Asymmetry* **1992**, *3*, 583−586. (d) Babin, J. E.; Whiteker, G. T. W.I.P.O. Patent 93/03830, 1992. (e) Nozaki, K.; Sakai, N.; Nanno, T.; Higashijima, T.; Mano, S.; Horiuchi, T.; Takaya, H. *J. Am. Chem. Soc.* **1997**, *119*, 4413−4423. (f) Masdeu-Bulto, A. M.; Orejon, A.; Castellanos, A.; Castillon, S.; Claver, C. *Tetrahedron: Asymmetry* **1996**, *7*, 1829−1834. (g) Whiteker, G. T.; Briggs, J. R.; Babin, J. E.; Barner, B. A. In *Catalysis of Organic Reactions*; Morrell, D. G., Ed.; Marcel Dekker: New York, 2003; p 359. (h) Cobley, C. J.; Gardner, K.; Klosin, J.; Praquin, C.; Hill, C.; Whiteker, G. T.; Zanotti-Gerosa, A.; Petersen, J. L.; Abboud, K. A. *J. Org. Chem.* **2004**, *69*, 4031−4040. (i) Cobley, C. J.; Klosin, J.; Qin, C.; Whiteker, G. *Org. Lett.* **2004**, *6*, 3277−3280. (j) Yan, Y. J.; Zhang, X. M. *J. Am. Chem. Soc.* **2006**, *128*, 7198−7202. (k) Axtell, A. T.; Klosin, J.; Abboud, K. A. *Organometallics* **2006**, *25*, 5003−5009. (l) Klosin, J.; Landis, C. R. *Acc. Chem. Res.* **2007**, *40*, 1251−1259. (m) Rubio, M.; Suarez, A.; Alvarez, E.; Bianchini, C.; Oberhauser, W.; Peruzzini, M.; Pizzano, A. *Organometallics* **2007**, *26*, 6428−6436. (n) Robert, T.; Abiri, Z.; Wassenaar, J.; Sandee, A. J.; Romanski, S.; Neudörfl, J.-M.; Schmalz, H.-G.; Reek, J. N. H. *Organometallics* **2010**, *29*, 478−483. (o) Wassenaar, J.; de Bruin, B.; Reek, J. N. H. *Organometallics* **2010**, *29*, 2767−2776. (p) Wang, X.; Buchwald, H. L. *J. Am. Chem. Soc.* **2011**, *133*, 19080−19083. (q) Gadzikwa, T.; Bellini, L.; Dekker, H. L.; Reek, J. N. H. *J. Am. Chem. Soc.* **2012**, *134*, 2860−2863. (r) Chikkali, S. H.; Bellini, R.; de Bruin, B.; van der Vlugt, J. I.; Reek, J. N. H. *J. Am. Chem. Soc.* **2012**, *134*, 6607−6616.

(4) (a) Clark, T. P.; Landis, C. R.; Freed, S. L.; Klosin, J.; Abboud, K. A. *J. Am. Chem. Soc.* **2005**, *127*, 5040−5042. (b) Klosin, J.; Landis, C. R. *Acc. Chem. Res.* **2007**, *40*, 1251−1259. (c) Watkins, A. L.; Hashiguchi, B. G.; Landis, C. R. *Org. Lett.* **2008**, *10*, 4553−4556. (d) McDonald, R. I.; Wong, G. W.; Neupane, R. P.; Stahl, S. S.; Landis, C. R. *J. Am. Chem. Soc.* **2010**, *132*, 14027−14029. (e) Watkins, A. L.; Landis, C. R. *Org. Lett.* **2011**, *13*, 164−167. (f) Adint, T. T.; Wong, G. W.; Landis, C. R. *J. Org. Chem.* **2013**, *78*, 4231−4238.

(5) Heck, R. F.; Breslow, D. F. *J. Am. Chem. Soc.* **1961**, *83*, 4023−4027.

(6) (a) Lazzaroni, R.; Uccello-Barretta, G.; Benetti, M. *Organometallics* **1989**, *8*, 2323−2327. (b) Casey, C. P.; Whiteker, G. T.; Melville, M. G.; Petrovich, L. M.; Gavney, J. A.; Powell, D. R. *J. Am. Chem. Soc.* **1992**, *114*, 5535−5543. (c) Casey, C. P.; Petrovich, L. M. *J. Am. Chem. Soc.* **1995**, *117*, 6007−6014. (d) Kranenburg, M.; van der Burgt, Y. E. M.; Kamer, P. C. J.; van Leeuwen, P. W. N. M.; Goubitz, K.; Fraanje, J. *Organometallics* **1995**, *14*, 3081−3089. (e) Lazzaroni, R.; Settambolo, R.; Uccello-Barretta, G. *Organometallics* **1995**, *14*, 4644−4650. (f) Casey, C. P.; Paulsen, E. L.; Beuttenmueller, E. W.; Proft, B. R.; Petrovich, L. M.; Matter, B. A.; Powell, D. R. *J. Am. Chem. Soc.* **1997**, *119*, 11817−11825. (g) Horiuchi, T.; Shirakawa, E.; Nozaki, K.; Takaya, H. *Organometallics* **1997**, *16*, 2981−2986. (h) van der Veen, L. A.; Boele, M. D. K.; Bregman, F. R.; Kamer, P. C. J.; van Leeuwen, P. W. N. M.; Goubitz, K.; Fraanje, J.; Schenk, H.; Bo, C. *J. Am. Chem. Soc.* **1998**, *120*, 11616−11626. (i) Casey, C. P.; Paulsen, E. L.; Beuttenmueller, E. W.; Proft, B. R.; Matter, B. A.; Powell, D. R. *J. Am. Chem. Soc.* **1999**, *121*, 63−70. (j) del Río, I.; Pàmies, O.; van Leeuwen, P. W. N. M.; Claver, C. *J. Organomet. Chem.* **2000**, *608*, 115−121. (k) van der Veen, L. A.; Keeven, P. H.; Schoemaker, G. C.; Reek, J. N. H.; Kamer, P. C. J.; van Leeuwen, P. W. N. M.; Lutz, M.; Spek, A. L. *Organometallics* **2000**, *19*, 872−883. (l) van der Slot, S. C.; Kamer, P. C. J.; van Leeuwen, P. W. N. M.; Iggo, J. A.; Heaton, B. T. *Organometallics* **2001**, *20*, 430−441. (m) van der Slot, S. C.; Duran, J.; Luten, J.; Kamer, P. C. J.; van Leeuwen, P. W. N. M. *Organometallics* **2002**, *21*, 3873−3883. (n) Freixa, Z.; van Leeuwen, P. W. N. M. *Dalton Trans.* **2003**, 1890−1901. (o) Watkins, A. L.; Landis, C. R. *J. Am. Chem. Soc.* **2010**, *132*, 10306−10317. (p) Kubis, C.; Sawall, M.; Block, A.; Neymeyr, K.; Ludwig, R.; Borner, A.; Selent, D. *Chem.—Eur. J.* **2014**, *20*, 11921−11931.

(7) (a) Watkins, A. L.; Landis, C. R. *J. Am. Chem. Soc.* **2010**, *132*, 10306−10317. (b) Tonks, I. A.; Froese, R. D.; Landis, C. R. *ACS Catal.* **2013**, *3*, 2905−2909.

(8) (a) Brown, J. M.; Kent, A. G. *J. Chem. Soc., Chem. Commun.* **1982**, 723−725. (b) Brown, J.; Kent, A. *J. Chem. Soc., Perkin Trans. 2* **1987**, 1597−1607.

(9) Schmidt, S.; Baráth, E.; Prommnitz, T.; Rosendahl, T.; Rominger, F.; Hofmann, P. *Organometallics* **2014**, *33*, 6018−6022.

(10) van der Slot, S.; Kamer, P.; van Leeuwen, P.; Heaton, B.; Iggo, J. *Organometallics* **2001**, *20*, 430−441.

(11) Deutsch, P.; Eisenberg, R. *Organometallics* **1990**, *9*, 709−718.

(12) Chan, A.; Huey-sheng, S. *Inorg. Chim. Acta* **1994**, *218*, 89−95.

(13) Abkai, G.; Schmidt, S.; Rosendahl, T.; Rominger, F.; Hofmann, P. *Organometallics* **2014**, *33*, 3212−3214.

(14) Nelsen, E. R.; Landis, C. R. *J. Am. Chem. Soc.* **2013**, *135*, 9636−9639.

(15) Tyler T. Adint, PhD Dissertation, University of Wisconsin-Madison, 2014, Appendix 1.

(16) The formation of acyl dicarbonyls appears to be thermodynamically favorable under these conditions, but this process requires consumption of 1 equiv of CO from solution. The concentration of **1** at the beginning of the reaction exceeds the estimated [CO] in solution, and because gas−liquid mixing is slow, the reaction becomes starved of gas as acyl dicarbonyl complexes are produced. This enables observation of the alkyl complexes, which do not require additional CO from solution.

(17) For selected examples, see (a) Heck, R. F. *J. Am. Chem. Soc.* **1968**, *90*, 5535−5538. (b) Cheng, J. C.-Y.; Daves, G. D., Jr. *Organometallics* **1986**, *5*, 1753−1755. (c) Zhu, G.; Lu, X. *Organometallics* **1995**, *14*, 4899−4904. (d) Zhang, Z.; Lu, X.; Xu, Z.; Zhang, Q.; Han, X. *Organometallics* **2001**, *20*, 3724−3728. (e) Williams, B. S.; Leatherman, M. D.; White, P. S.; Brookhart, M. *J. Am. Chem. Soc.* **2005**, *127*, 5132−5146. (f) Yu, J.-Y.; Kuwano, R. *Angew. Chem., Int. Ed.* **2009**, *48*, 7217−7220. (g) Ogiwara, Y.; Tamura, M.; Kochi, T.; Matsuura, Y.; Chatani, N.; Kakiuchi, F. *Organometallics* **2014**, *33*, 402−420.

(18) (a) Komiya, S.; Yamamoto, A. *J. Chem. Soc., Chem. Commun.* **1974**, 523b−524. (b) Komiya, S.; Yamamoto, A. *J. Organomet. Chem.* **1975**, *87*, 333−339. (c) Abrams, M. L.; Foarta, F.; Landis, C. R. *J. Am. Chem. Soc.* **2014**, *136*, 14583−14588.

(19) Fryzuk, M. D. *Inorg. Chem.* **1982**, *21*, 2134−2139.

(20) Beach, N. J.; Knapp, S. M. M.; Landis, C. R. *Rev. Sci. Instrum.* **2015**, *86*, 104101−104109.

(21) Hoops, S.; Sahle, S.; Gauges, R.; Lee, C.; Pahle, J.; Simus, N.; Singhal, M.; Xu, L.; Mendes, P.; Kummer, U. *Bioinformatics* **2006**, *22*, 3067−3074.

DOI: 10.1021/jacs.5b09858
J. Am. Chem. Soc. 2015, 137, 14208−14219

(22) The WiHP-NMRR uses dinitrogen for injection of the substrate. This results in some initial degassing of dissolved CO, such that even with active mixing there is a brief time of approximately 2 min where the dissolved CO concentration is lower than the equilibrium value. As a result the ratio of acyl dicarbonyls (5:1) observed is slightly lower than the limiting catalytic kinetic selectivity (12:1) at the same temperature and pressure.

DOI: 10.1021/jacs.5b09858
J. Am. Chem. Soc. 2015, 137, 14208−14219